



Research report

Chronic administration of aluminum–fluoride or sodium–fluoride to rats in drinking water: alterations in neuronal and cerebrovascular integrity

Julie A. Varner^{a,*}, Karl F. Jensen^b, William Horvath^c, Robert L. Isaacson^a^a *Psychology Department, Binghamton University, Binghamton, NY, USA*^b *Neurotoxicology Division, NHEERL, EPA, Research Triangle Park, NC, USA*^c *Chemistry Department, Binghamton University, Binghamton, NY, USA*

Accepted 29 October 1997

Abstract

This study describes alterations in the nervous system resulting from chronic administration of the fluoroaluminum complex (AlF_3) or equivalent levels of fluoride (F) in the form of sodium–fluoride (NaF). Twenty seven adult male Long–Evans rats were administered one of three treatments for 52 weeks: the control group was administered double distilled deionized drinking water (ddw). The aluminum-treated group received ddw with 0.5 ppm AlF_3 and the NaF group received ddw with 2.1 ppm NaF containing the equivalent amount of F as in the AlF_3 ddw. Tissue aluminum (Al) levels of brain, liver and kidney were assessed with the Direct Current Plasma (DCP) technique and its distribution assessed with Morin histochemistry. Histological sections of brain were stained with hematoxylin & eosin (H&E), Cresyl violet, Bielschowsky silver stain, or immunohistochemically for β -amyloid, amyloid A, and IgM. No differences were found between the body weights of rats in the different treatment groups although more rats died in the AlF_3 group than in the control group. The Al levels in samples of brain and kidney were higher in both the AlF_3 and NaF groups relative to controls. The effects of the two treatments on cerebrovascular and neuronal integrity were qualitatively and quantitatively different. These alterations were greater in animals in the AlF_3 group than in the NaF group and greater in the NaF group than in controls. © 1998 Elsevier Science B.V.

Keywords: Aluminum; Fluoride; Neurotoxicity; Chronic; Cerebrovasculature; Neocortex; Hippocampus; Rat; Amyloid

1. Introduction

Epidemiological studies have raised the possibility that prolonged exposure to aluminum (Al) in drinking water, perhaps as low as 0.1 ppm, may represent a risk factor for aging-related neurological impairments [4,23,24,33,34,42,47,48,52,60,71,72,75,76,80]. In determining the effects of chronic exposure to Al in the drinking water it is important to consider the factors that enhance or inhibit the bioavailability of Al and its effects on the nervous system [1,19,25,30]. One such factor is the nature of the Al complex and its speciation after ingestion. Schroeder et al. [61] has hypothesized that when fluoride (F) and Al are both present in drinking water they will form fluoroaluminum complexes (AlF_3) in the stomach that, compared to their ionic forms, exhibit increased transport into the

bloodstream and likely across the blood–brain barrier (BBB). This possibility was investigated by Varner et al. [78] who examined the behavioral and morphological effects of 45 weeks ingestion of the AlF_3 in double-distilled water provided for drinking. They administered either 0.5 ppm, 5.0 ppm, 50 ppm AlF_3 in the drinking water to male Long–Evans rats 4–5 months of age. One of their most remarkable findings was that animals administered the lowest dose of AlF_3 (0.5 ppm) exhibited a greater susceptibility to illness and higher mortality than animals administered higher levels (5 ppm, 50 ppm) of Al. The reasons for the selective high mortality rate following this dose are unknown. Histological examination of the brains of the Al-treated animals revealed a significant reduction in the number of cells in areas CA1 and CA3 of the hippocampus in the AlF_3 -treated groups relative to the control group, but no differences were found among the groups of rats receiving different concentrations of AlF_3 . Qualitatively, two patterns of anomalies were observed in the AlF_3 groups: (1) argentophilic cells prominent in CA1, CA3, dentate

* Corresponding author. Lineberry Research Associates, P.O. Box 14626, Research Triangle Park, NC 27709. Fax: +1-919-547-0974; E-mail: jvarner@lineberryresearch.com

gyrus, and neocortex, and (2) increased aluminum-fluorescence present throughout the brain and cerebral blood vessels. The latter histological pattern was consistent with the finding that the level of Al in the brains of the AlF_3 animals was almost double that of the control animals as indicated by the Direct Current Plasma (DCP) technique. Although dramatic behavioral differences were not observed during the ingestion of AlF_3 , the increased Al content of the brain together with the observed morphological anomalies are likely results of the enhanced access of Al to the cerebrovasculature and the brain.

One possible reason for the increased infections and mortality of animals in the 0.5 ppm AlF_3 group rests on the assumption that the toxic agent of importance was the fluorine and its absorption or its effects were antagonized by the higher levels of Al found in the higher doses of AlF_3 . Al, at certain levels, has the capacity to decrease F uptake and reduce signs of F toxicity [77,78]. If tissue F levels were the primary determinant in the increased infections and mortality, then the lower amount of Al at the 0.5 ppm level of AlF_3 may have been insufficient to reduce F uptake. A number of the other possibilities, however, may also account for the severity of effects occurring in the lowest dose group. To help understand the results of this earlier experiment, we undertook the present study to compare the effects of the 0.5 ppm AlF_3 with a comparable level of F administered alone in the form of NaF. A concentration (2.1 ppm) of NaF was used that contained the same amount of F as 0.5 ppm AlF_3 .

As in the original AlF_3 studies by Varner et al. [77,78], the Al levels in samples of the brain, kidney, and liver were determined by the DCP and the pattern of distribution of Al was assessed histochemically in brain, kidney, liver and spleen. Morphological alterations were characterized in the hippocampus and neocortex. Cerebrovascular integrity was assessed with IgM immunostaining. Since Al may influence amyloid deposition, we also compared the pattern of β -amyloid and amyloid A immunostaining. Pathological evaluations of kidney, liver and spleen were also conducted.

2. Materials and methods

2.1. Animals

Twenty-seven male, Long–Evans rats, 3.5 to 4.5 months of age at the start of the treatment schedule were used. The animals were divided into three groups (nine rats/group) and individually housed throughout the experiment. All subjects were from a stock colony at Binghamton University and maintained on a 12:12 h light:dark schedule. Food was provided ad libitum except when testing was conducted in a behavioral task that required food deprivation.

During such periods, food was removed from the cages for 18–20 h prior to testing (weeks 24 to 27). Water was available ad libitum. Prior to the beginning of treatment, animals had access to tap water which had non-detectable (< 50 ppb) Al levels. Depending on group assignment, treatment consisted of double-distilled drinking water (ddw) buffered to a pH of 7.0, 0.5 ppm AlF_3 in ddw or 2.1 ppm NaF, with the latter two treatments having the same F molar concentration (see Section 2.2). Exposure to the treated water continued for 52 weeks. Body weights were recorded weekly for the first 10 weeks and then biweekly throughout the remainder of the experiment.

2.2. Preparation of AlF_3 and NaF solutions

The 2.1 ppm concentration of NaF was selected to provide the same F^- as available from AlF_3 and took into consideration the method of producing the AlF_3 solution, i.e., the addition of the aluminum nitrate and sodium–fluoride (NaF) to ddw in a mole ratio of 1:6 (Al:F) as well as the variety of Al species formed. Stoichiometric calculations indicate the predominant species formed to be AlF_3 and AlF_4^- [82] and that a level of 2.1 ppm of NaF provides a comparable level of F^- as present in the drinking water of AlF_3 group. In this paper, the term AlF_3 will be used to represent all of the species formed.

2.3. Tissue samples

Brain, kidney, liver, and spleen were recovered for processing from all of the animals that died during the course of the study. At the termination of the experiment, the surviving animals were sacrificed with a lethal dose of sodium pentobarbital (Nembutal, Abbott Laboratories). The brains were removed and a 6 mm coronal block corresponding to a region extending from 2 mm to 8 mm from bregma was immersed in 10% formalin. The remaining frontal and caudal blocks of the brain, as well as blocks of kidney and liver, were frozen for DCP analysis of the Al content [82]. Additional blocks of kidney, liver and spleen were immersed in 10% formalin for histological processing.

2.4. Aluminum tissue levels

The amount of Al in samples of brain and kidney were determined by the method of Horvath and Huie (1995) for analysis of high fat biological tissues. Tissue samples were homogenized and digested with Utrex HNO_3 and fed through a nebulizer into an atomic emission spectrometer (Fisons model SS7). An analytic mode was used to detect emission intensity at 396.152, corresponding to Al. The unit was calibrated to a resolution of 0.006 nm and detection limit of 2 ppb. This approach detects both free and bound Al.

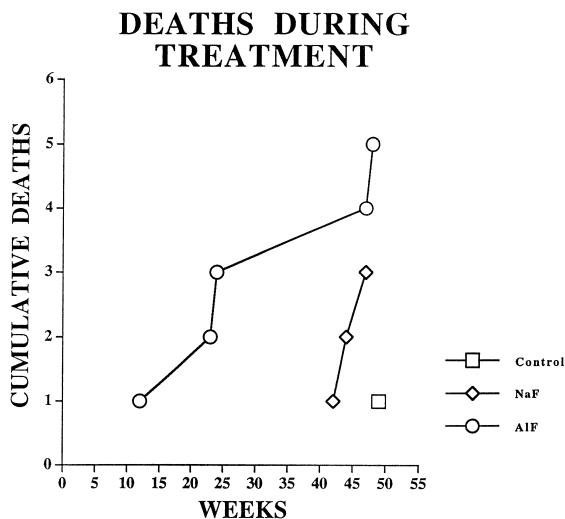


Fig. 1. Cumulative deaths over the course of the experiment.

2.5. Histology

Fixed tissue samples were embedded in paraffin and sectioned at 8 μm . Sections of brain, kidney and spleen were stained with hematoxylin & eosin (H&E) or with the Morin aluminum-fluorescence method [14] with a Cresyl violet counterstain. Additional coronal sections of the brain were stained with a modified Bielschowsky silver stain or immunohistochemically labeled with antisera specific for IgM, β -amyloid, or amyloid A.

All sections processed for immunohistochemistry underwent the same initial steps used in preparing the paraffin-embedded tissue for processing, sectioning, deparaffinization, rehydration. All incubations were carried out in a humidified chamber at room temperature and except where noted all washes were carried out in Tris buffer, pH = 7.2 (TBS). To confirm that the presence of labeling was due to the primary antibody, additional slides were processed without the primary antibody, without the secondary antibody or without either the primary or secondary antibodies. Additional sections underwent a methanol/hydrogen peroxide pretreatment to abolish endogenous peroxidase activity. All secondary antibodies were from Elite ABC Kits, Vector Laboratories.

For immunolabeling with β -amyloid antisera, slides were pretreated with concentrated formic acid for 3 min [41], rinsed, incubated with 10% blocking serum (10% normal horse serum and TBS) for 1 h, and then incubated overnight with a primary antisera specific for β -amyloid (dilution 1:100, mouse monoclonal, Dako). Sections were then washed, incubated 1 h with the biotinylated secondary antibody, washed again and then incubated with the avidin-biotin horseradish peroxidase complex for 30 min. The sections were then washed and the peroxidase label was visualized with cobalt-nickel intensified diaminobenzidine. The procedure for amyloid A antisera (dilution 1:100, monoclonal mouse, Dako) was the same as the

procedure for β -amyloid antisera, except that the pretreatment with formic acid was omitted. The procedure for the IgM antisera (dilution 1:100, rabbit polyclonal, Jackson ImmunoResearch) was the same as for amyloid A except 0.1 M phosphate buffer (pH = 7.2) was used instead of TBS.

2.6. Morphological evaluations

All counts and ratings were conducted by three individuals, two of whom were always blind to the treatment of the rats from whom the tissues came. For the distribution of Al-fluorescence demonstrated with the Morin method, ranking was based on overall intensity and extent of fluorescence across a $400 \times 400 \mu\text{m}$ field in specific regions of brain, kidney and spleen. Three grades of Morin produced fluorescence (1 = low, 2 = moderate, 3 = high).

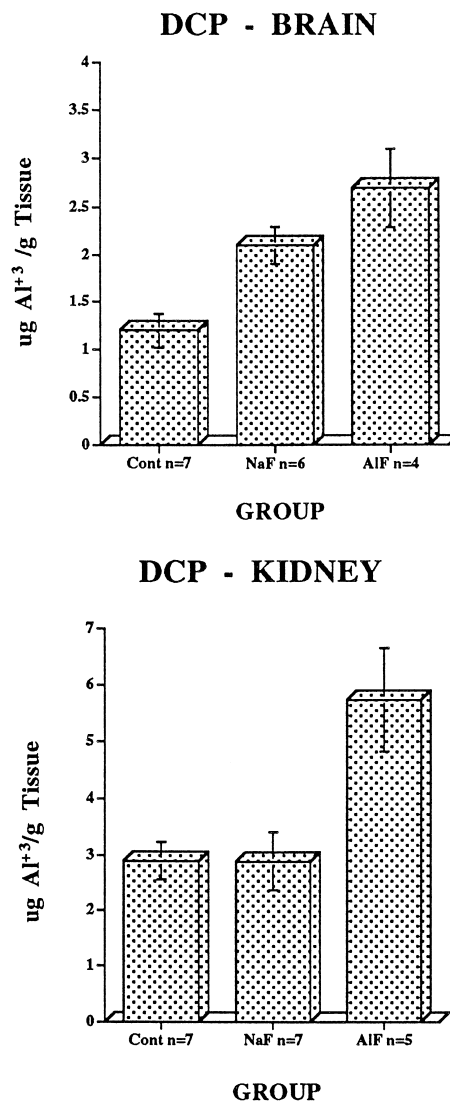


Fig. 2. The amount of aluminum (μm) in brain and kidney tissue (g) as determined by DCP analysis.

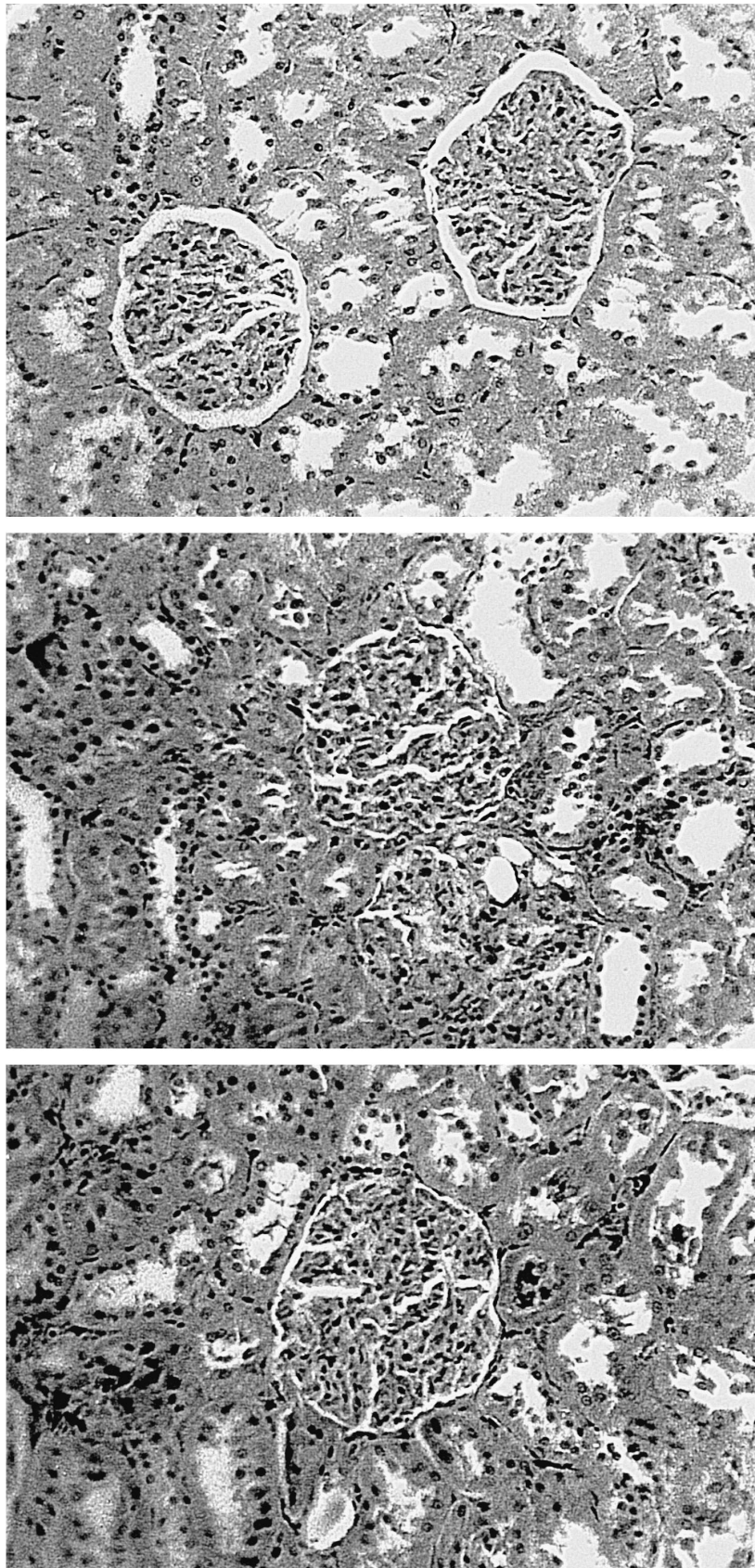


Fig. 3. Photomicrographs of the glomeruli of the kidney. Note Bowmans space surrounding the glomerulus of the control and the infiltration of this space in the treated groups. Magnification = $250\times$. Row 1 = Control, Row 2 = NaF, Row 3 = AlF_3 .

Ranking of immunohistochemical label for IgM, β -amyloid, and amyloid A was based on the amount of immunoreactivity present in $800 \times 800 \mu\text{m}$ fields of the particular region of interest (0 = none, 1 = low, 2 = high).

The assessment of neuronal integrity focused on the superior parietal cortex, hippocampus and dentate gyrus from coronal sections taken at levels in which the dorsal, but not ventral, hippocampus was present. Observations of H&E-stained sections were made in a $250 \times 250 \mu\text{m}$ area of the particular region of interest. The following characteristics were considered indicative of neuronal injury in H&E-stained sections: the number of neurons having clumped and darkened chromatin, hyperchromasia, extensive vacuolation, pyknosis, 'ghost-like' appearance (i.e., well demarcated neuronal outlines with faint, barely detectable structure). These characteristics are traditionally

used as indices of necrosis. A rating of 0 was given to an area when few or no cells in the area showed these characteristics. A rating of 1 was given when between 10 and 50% of the cells showed signs of abnormality. A rating of 2 was given when over half of the neurons in the field showed signs of abnormalities.

Neurons were rated and counted as normal if they were normal in shape with dispersed chromatin and prominent nuclei. The assessment of the damaged areas is expressed as observed frequencies of normal cells or cells with various degrees of abnormality. All neocortical layers in each hemisphere were examined. This rating was then converted to percentages and presented as such in the figures. Percentages are based on the number of observed frequencies in each category divided by the group total (n) and then multiplied by 100. For example, if in a group of

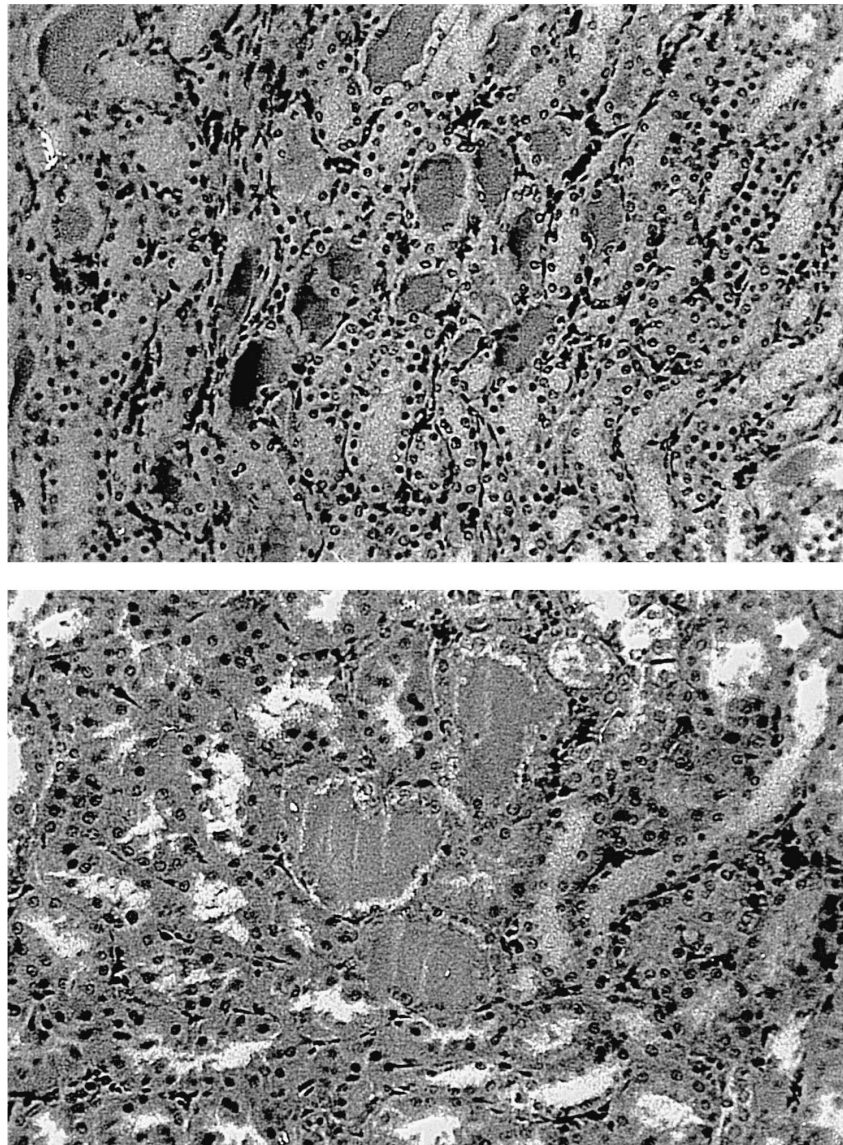


Fig. 4. Photomicrographs of protein deposits in the kidney of only the treated groups. Magnification = $250 \times$. Row 1 = Control, Row 2 = NaF, Row 3 = AlF_3 .

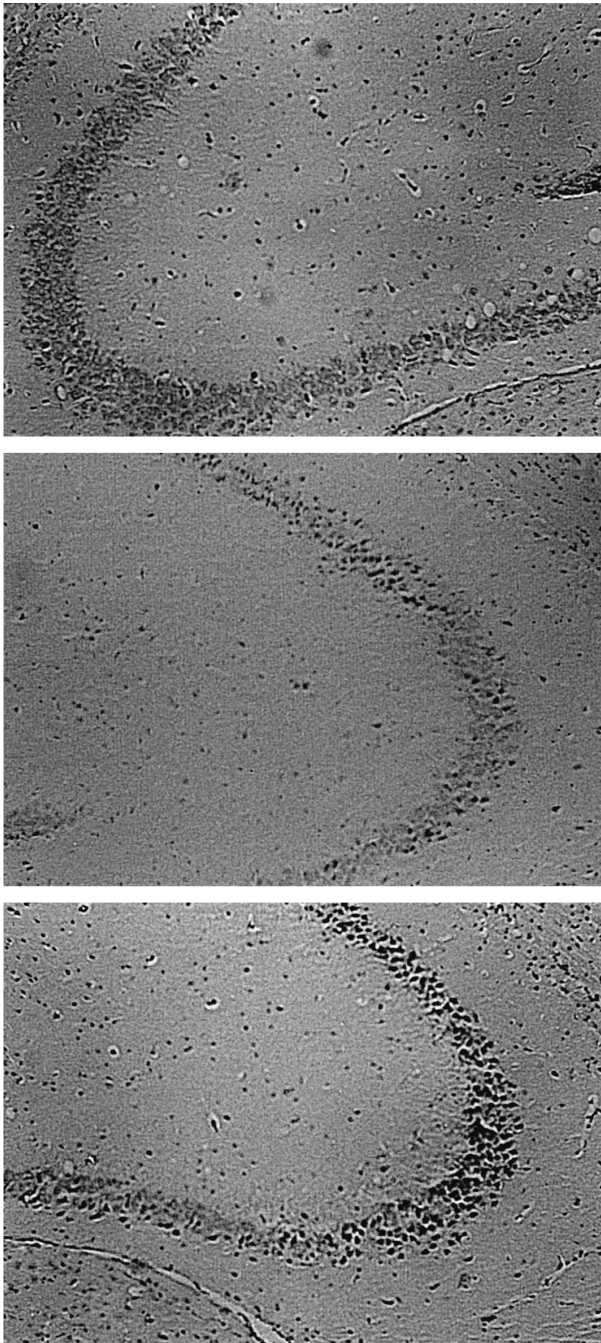


Fig. 5. Photomicrographs illustrating examples of ratings of neuronal injury in the hippocampus. Row 1 = Control, Row 2 = NaF, Row 3 = AlF₃.

10 animals in which only 2 subjects meet a specified criterion for a certain category (i.e., normal cells), then the percent occurrence for that category would be 20%.

The density of neurons in layers 2, 3, 4, 5, and 6 of the neocortex on both sides of the brain were counted in sections stained with Cresyl violet stain using a 350 × 200 μm field for each sample. An image from a Magnavox video camera mounted on Nikon microscope was displayed on Sony Trinitron television and a clear plastic

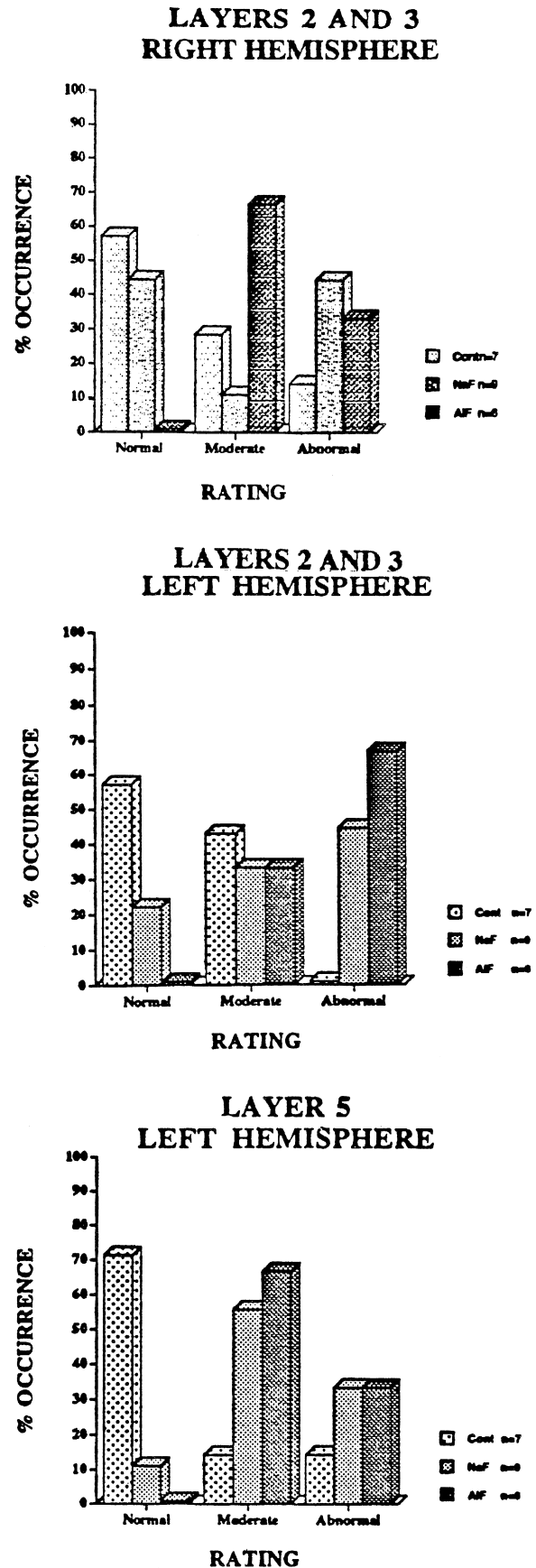


Fig. 6. Frequency of neuronal abnormalities in the neocortex. Data are expressed as percent of occurrences within the rating scale.

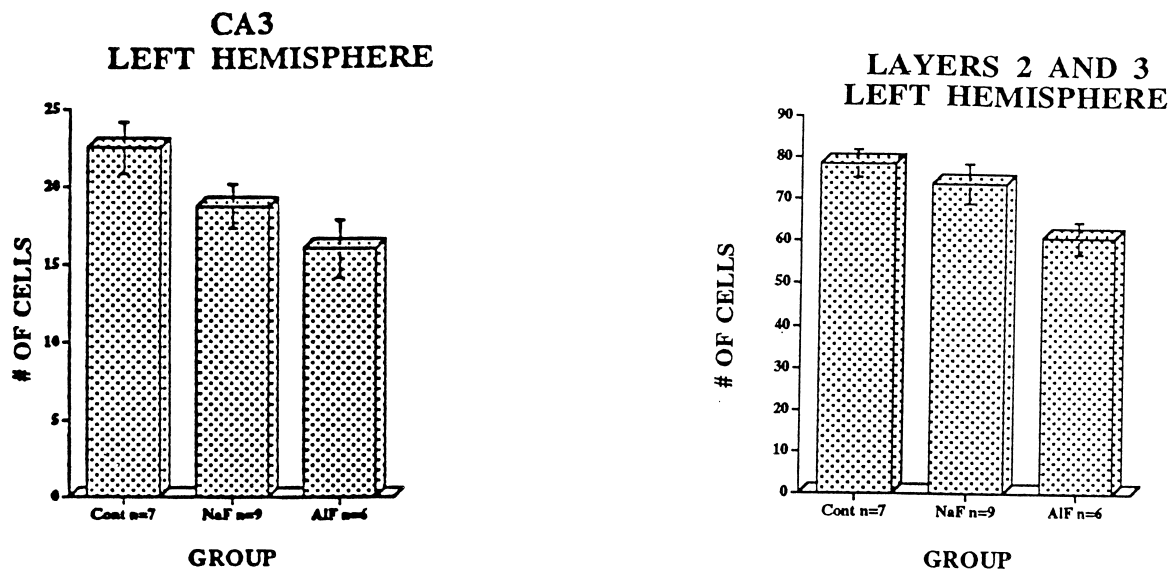


Fig. 7. Alterations in neuronal density in CA3 of the hippocampus of the left hemisphere.

template with a grid was placed on the display screen to demarcate the sample area for the cell counts. The neurons of CA1, CA3, and CA4 were counted in sections stained with the modified Bielschowsky silver stain. For these areas, cell counts were made directly as projected from the Nikon microscope with an ocular grid and a sample field of $250 \times 250 \mu\text{m}$.

Sections of kidney, liver, and spleen were stained with H&E and details of preparation as well as the rating scales were the same as described above.

2.7. Statistics

One-way ANOVA was used to determine group differences in cell counts and DCP. Post hoc analyses, when necessary, were conducted by Fisher LSD. Chi square (X^2) contingency tables were used for analyses of data from rating scales.

3. Results

3.1. General condition of the animals

A progressive general decline in appearance of the AIF₃ animals was noted throughout the experiment. In addition to the yellowing of the hair that occurs with age, the hair of animals in the AIF₃ group became sparse revealing the underlying skin which was dry, flaky, and of a copper color. Although the body weights did not differ among the groups, there was a greater number of deaths in the AIF₃ group than in the control group ($X^2(1) = 4$, $p = 0.05$, Fig. 1).

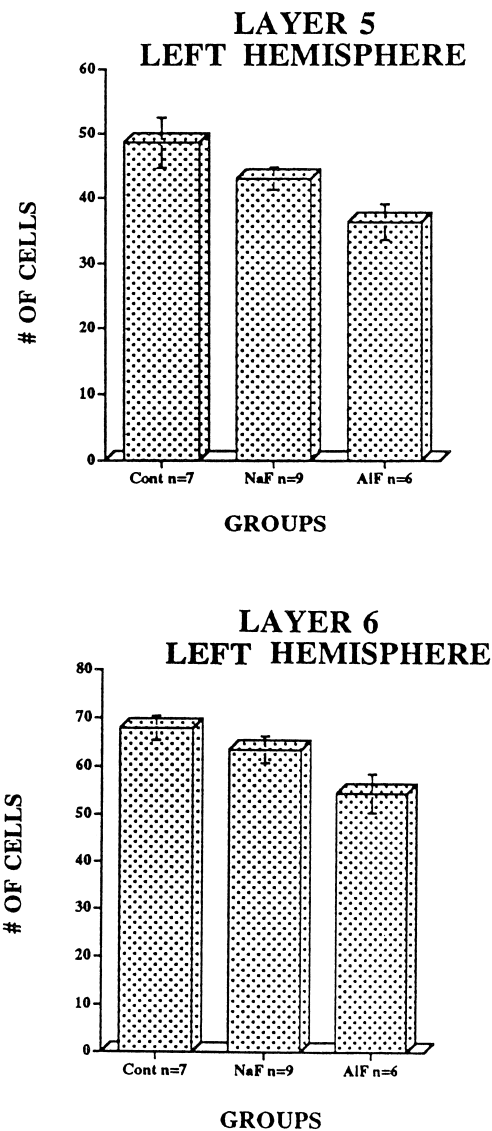


Fig. 8. Alterations in cell density of the neocortex.

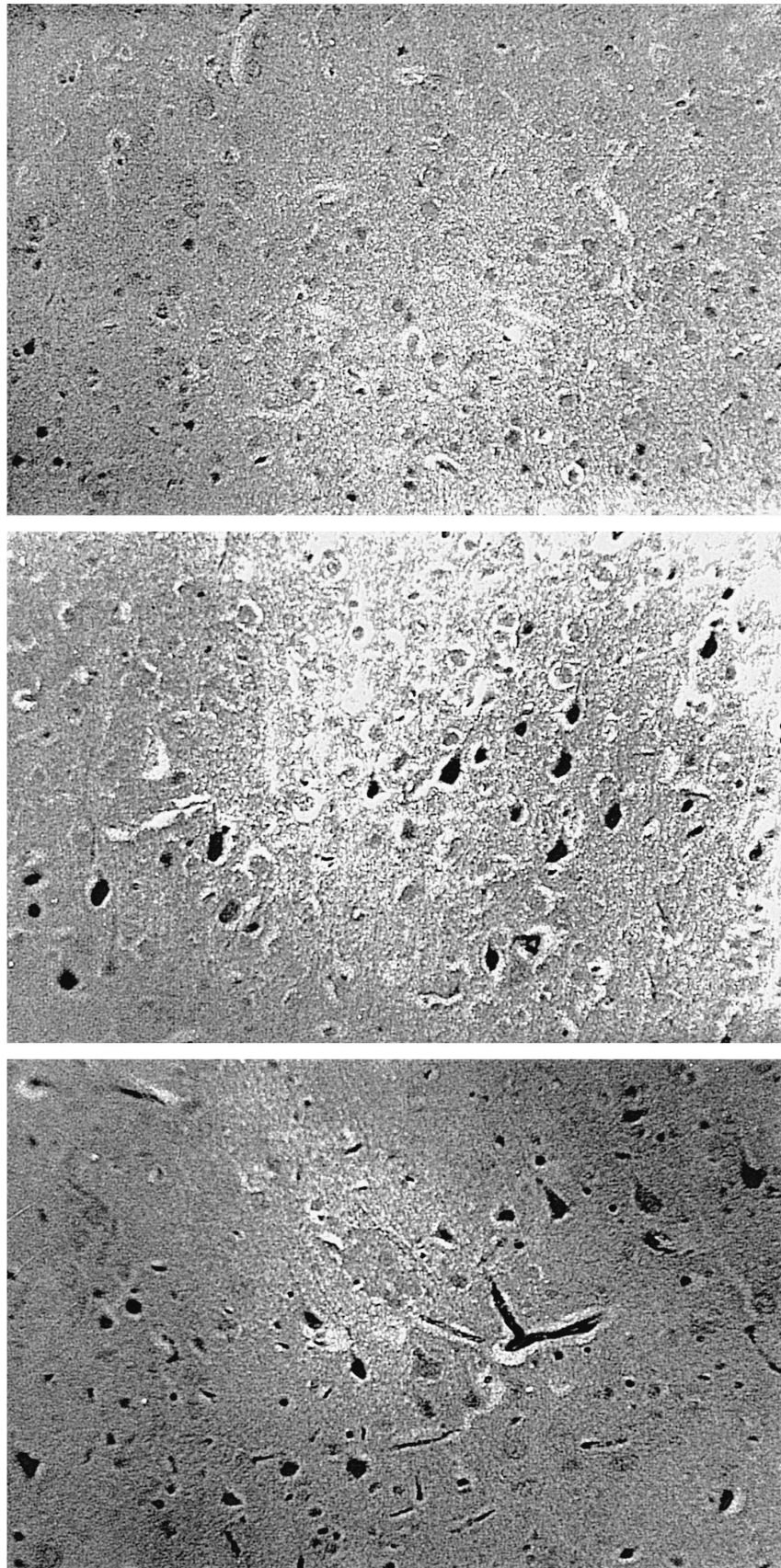


Fig. 9. Photomicrographs IgM immunoreactivity in the cortex of the right hemisphere. Magnification = $250\times$. Row 1 = Control, Row 2 = NaF, Row 3 = AlF_3 .

3.2. Aluminum levels in DCP tissue samples

The brains of the AlF_3 and NaF groups had higher levels of Al compared to controls ($F(2,14) = 9.793$, $p < 0.01$, Fisher LSD, $p < 0.05$, Fig. 2). The kidneys of the AlF_3 group exhibited elevated Al levels compared to both the control and NaF groups [$F(2,16) = 7.265$, $p < 0.01$] (Fisher LSD, $p < 0.05$, Fig. 2). There was no difference between the treatment groups in Al levels in the liver.

3.3. Distribution of aluminum in sections stained with Morin method

Al-fluorescence in sections of the brain was exclusively associated with vasculature where it occurred as deposits within the lumen, within endothelial cells, and in the adventitia. This type of Al-fluorescence was also detected in the brains of control animals as well as those of animals receiving either treatment. In all groups there were consistent treatment-related differences in the intensity and extent of Al-fluorescence. Greater amounts of fluorescence were observed to occur in the deeper layers of the neocor-

tex and in the hippocampus of the left hemisphere than in the right. Ratings by observers blind to the experimental groups confirmed the AlF_3 group exhibited greater fluorescence in layer 6 of the left hemisphere than the controls [$X^2(2) = 6.741$, $p < 0.03$]. Greater Al-fluorescence also occurred in layer 5 of the left hemisphere of the AlF_3 group compared to the same region of brains from the NaF group [$X^2(2) = 7.187$, $p < 0.03$] and controls [$X^2(2) = 9.479$, $p < 0.01$]. CA3 and CA4 regions of the hippocampus of the left hemisphere of the brains from the AlF_3 group also exhibited increased fluorescence compared to controls [$X^2(2) = 6.741$, $p < 0.04$].

In the kidney, while some Al-fluorescence was detected within glomeruli and tubules, substantially more fluorescence was associated with vasculature. The only treatment-related increase in Al-fluorescence detected in the kidney was that associated with the vasculature and reached significant amounts only when the AlF_3 group was compared with controls [$X^2(2) = 13$, $p < 0.01$].

In the liver, Al-fluorescence could be detected in the sinuses and blood vessels of all animals. The only significant difference between treatment groups, however, was a

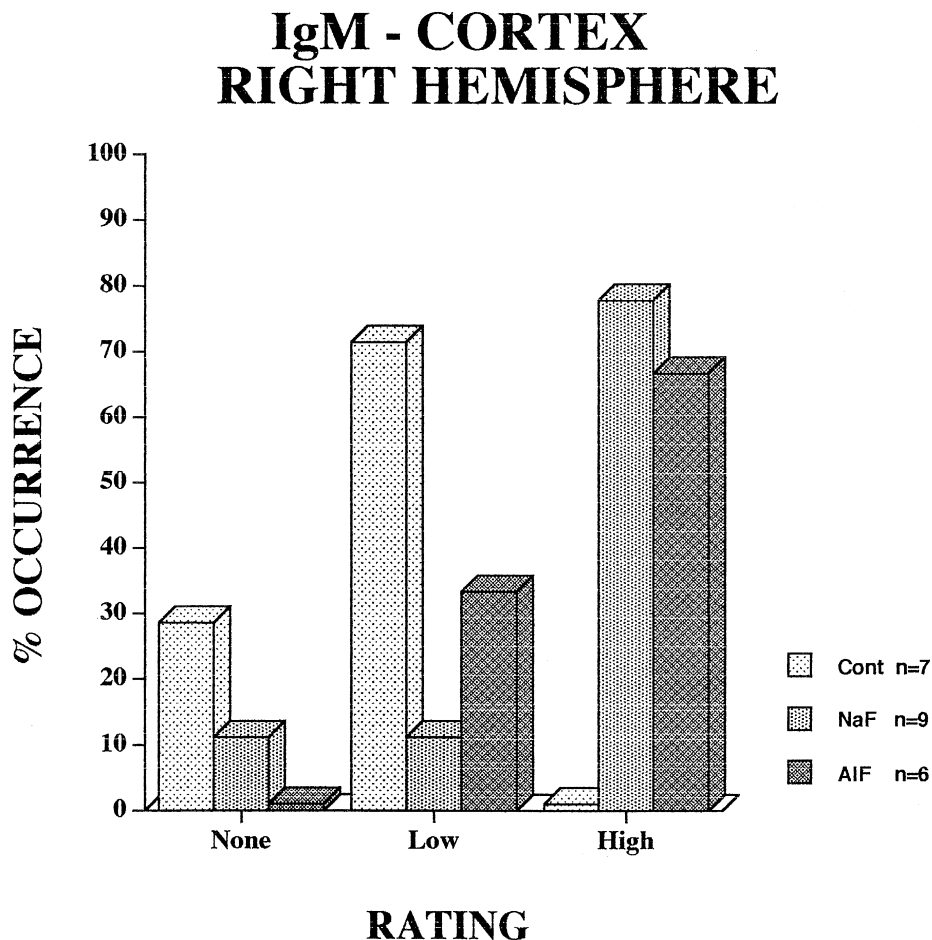


Fig. 10. Alterations of IgM immunolabeling in the neocortex. Data are expressed as percent of occurrences within the rating scale.

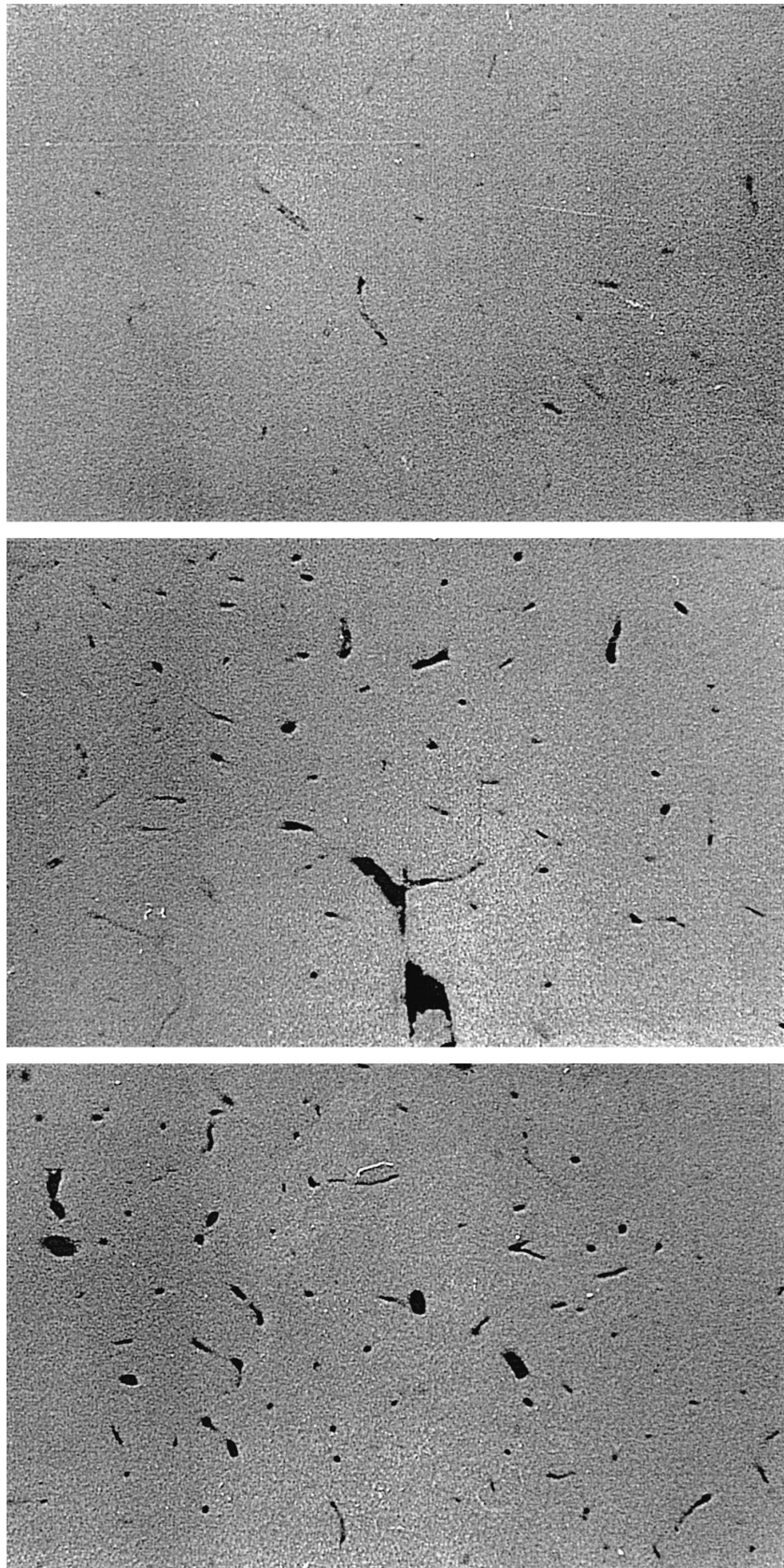


Fig. 11. Photomicrographs of β -amyloid immunoreactivity in the vessels of the thalamus of the right hemisphere. Magnification = $250\times$. Row 1 = Control, Row 2 = NaF, Row 3 = AlF_3 .

reduction of Al-fluorescence associated with the vasculature in the NaF group compared to the control group [$X^2(2) = 7.143$, $p < 0.03$].

3.4. Morphological assessments of kidney, liver and spleen

In the kidney, glomerular hypercellularity and mesangial proliferation was apparent in animals from both the NaF and AlF_3 treatment groups (Fig. 3). Congruent with the glomerular changes was deposition of protein in the tubules (Fig. 4). There was a significant increase in the extent of monocyte infiltration in the animals treated with AlF_3 compared to controls [$X^2(2) = 8.31$, $p < 0.05$].

No differences among the groups were observed in the liver. All hepatocytes appeared normal in shape displaying the typical rounded appearance with demonstrable nuclei and chromatin. Sinusoids, venules, and vessels all appeared normal.

While there was some infiltration of the marginal zones of the spleen by reactive lymphocytes in both AlF_3 and NaF groups, no consistent pattern of treatment-related pathological alterations was apparent.

3.5. Morphological assessment of neuronal integrity

Neuronal integrity was assessed in the neocortex and hippocampus and particular attention was paid to possible hemispheric localization of effects. There were more moderately damaged and grossly abnormal cells in areas CA1 and CA4 of the right hippocampus in the AlF_3 group than in the control group [$X^2(2) = 6.533$, $p < 0.04$; $X^2(2) = 7.098$, $p < 0.03$] (Fig. 5). The differences between these groups in the left hippocampal region were not statistically significant.

In neocortical layers 2 and 3 of the right hemisphere, a significant difference was found between the AlF_3 and the NaF groups. The AlF_3 group had more moderately damaged cells than the NaF group which had more normal cells [$X^2(2) = 6.11$, $p < 0.04$] (Fig. 6). In neocortical layers 2 and 3 of the left hemisphere, the AlF_3 group had more abnormal cells [$X^2(2) = 8.171$, $p < 0.02$] than did controls. Corresponding increases in the frequency of normal appearing cells were observed in neocortex of control animals. No differences among the groups were found in the cells of layer 6 in either hemisphere.

In addition to differences in the frequency of abnormal neurons there were also differences between the treatment groups in neuronal density in the hippocampus and neocortex. In the hippocampus, neuronal density was decreased in area CA3 in the left hemisphere of the AlF_3 group relative to controls [$F(2,19) = 3.631$, $p < 0.05$; Fisher LSD post hoc, $p < 0.05$] (Fig. 7). No significant differences in neuronal density were found among groups in areas CA1 and CA4 in either hemisphere. There was a significant decrease in neuronal density of neocortical layers 2 and 3 in the left hemisphere of AlF_3 group relative to the con-

trols and to the NaF groups [$F(2,19) = 3.981$, $p < 0.04$, Fisher LSD $p < 0.05$] (Fig. 8). Significant reductions of cell density were found in layers 5 and 6 of the AlF_3 group compared to controls in the left hemisphere [$F(2,19) = 4.137$, $p < 0.03$; $F(2,18) = 4.307$, $p < 0.03$]. No differences were detected in layer 4 of the left hemisphere among the groups. No significant differences were found among any of the groups in the right hemisphere of any layers of neocortex.

3.6. Integrity of the cerebrovasculature

In control animals, the localization of IgM was largely restricted to the vascular lumen (Fig. 9), indicative of the

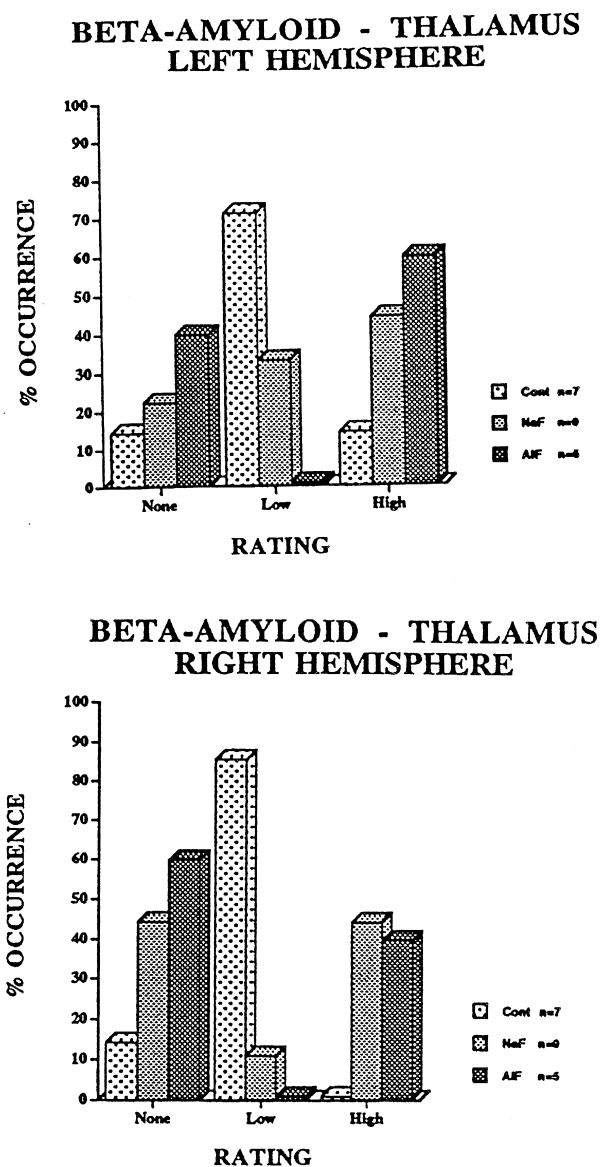


Fig. 12. Alterations in β -amyloid immunolabeling in the lateral posterior thalamus. Data are expressed as percent of occurrences within the rating scale.

integrity of the BBB to IgM. Staining of the neuronal parenchyma in the AlF₃ and NaF groups was significantly increased in the right hemisphere [AlF₃: $X^2(2) = 7.252$, $p < 0.03$, NaF: $X^2(2) = 9.905$, $p < 0.01$] (Fig. 10). No differences were found among the groups in the IgM immunoreactivity in the left hemisphere. Minor amounts of IgM immunostaining was detectable in the hippocampus and dentate gyrus but there were no significant differences among the groups.

Differences in the amount of immunoreactivity for β -amyloid relative to that for amyloid A were most prominent in the vasculature of the dorsal thalamus (Figs. 11 and 12). The control group had few instances of immunoreactivity while the tissue of animals from the AlF₃ group demonstrated a bimodal distribution of reaction product—the animals had an absence of reaction product staining or a high level. A significant difference was found between the AlF₃ and the control group in the lateral posterior thalamic areas in both hemispheres [left: $X^2(2) = 6.171$, $p < 0.05$; right: $X^2(2) = 8.914$, $p < 0.01$]. The NaF group also differed significantly from the control group in the right lateral posterior thalamic area: the controls demonstrated low immunoreactivity while rats in the NaF group had either no or high levels of immunoreactivity [$X^2(2) = 9.266$, $p < 0.01$].

4. Discussion

As found in our previous study [77,78], a high mortality rate resulted from the chronic administration of 0.5 ppm of AlF₃ to rats in their drinking water. Since, in the present study, the administration of NaF alone did not produce a similar mortality rate, this effect does not appear to be directly related to F intake. Additional characterization will be necessary to determine if the role of differential injury to several organ systems contributed to the increased mortality at the lower doses of AlF₃.

The AlF₃ animals presented an unusual appearance; their hair was sparse and the underlying skin was discolored. The presence of a copper color hypermelanosis may be indicative of several disease conditions among which is chronic renal failure [10]. Histological evidence of glomerular distortions and other signs of kidney disorders were found in animals in both the AlF₃ and NaF groups, although expressed differently. It is possible that physiological alterations in kidney function, not related to histological evidence of injury, were greater in the AlF₃ group than the NaF group. The overall Al content of the kidneys in the AlF₃ group was nearly double that found in the NaF and control groups. Since the kidney is critical to the elimination of both Na and Al, such alterations may have influenced the body burden of these elements, detoxification in general, as well as homeostasis of a variety of important ions, such as calcium. It is also possible that the

skin changes seen in the present experiment and in our previous study in the 0.5 AlF₃-treated animals came from disorders of organ systems other than the kidney.

Both the AlF₃ and NaF groups had increased brain Al levels relative to controls. The Al level in the NaF group was double that of controls and the Al level in the AlF₃ group was even greater. The Al detected in the controls and NaF groups is most likely due to the presence of this element in the rat chow. Reported estimates of the Al content in Purina Rodent Laboratory Chow range from 150 ppm to 8300 ppm Al [22] (L. Goldberg, Personal communication, 1994; W.J. Horvath, Personal communication, 1994). These data indicate that normal rat chow provides the Al availability for all animals, including the controls. Flouride also commonly occurs in food and water. They are almost completely and quickly absorbed from the gastrointestinal tract [38,44,46,69]. In the present experiment the AlF₃ in the drinking water was prepared to form optimally a fluoroaluminum species capable of crossing the gut and vascular barriers. It is possible that the NaF-treated group was able to form some amount of a AlF₃ also capable of becoming bioavailable.

In general, the reduction of neuronal density in the neocortex of the left hemisphere was more prominent in the AlF₃ group than the NaF and control groups. Cellular abnormalities in the form of chromatin clumping, enhanced protein staining, pyknosis, vacuolation, and the presence of ghost-like cells were also more common in the AlF₃ group in the left hemisphere. These alterations are consistent with the previously reported finding of marked argentophilic pyramidal neurons in layers 3 and 5 of the neocortex and in the pyramidal cell layers of the hippocampus in cats administered intracerebroventricular Al-chloride [13]. In the present study, vascular Al-fluorescence was more pronounced throughout most structures of the left hemisphere of the AlF₃ group. The hippocampus was an exception to these conditions, abnormalities were found only in areas CA1 and CA4 of the right hemispheres of both treatment groups. In addition, the right hippocampus had higher levels of Al-induced fluorescence than the left.

A variety of cellular mechanisms could underlie the association between regional Al accumulation and regional patterns of neuronal injury. These include transferrin transport (Tf), calcium homeostasis and second messenger systems, alterations in neuronal cytoskeleton, and alterations in the cerebrovasculature. Tf transports certain metals into the cells by a receptor-mediated endocytosis at the Tf-receptor complex located on plasma membranes [49,58]. It has been shown that Al binds to Tf and can gain access to cells in the brain via the Tf-receptor system [22,58]. Neurotoxic reactions to Al may also result from disruption of ion homeostasis and second messenger systems, in particular G-proteins [29,35,39,50,51,54,59,64,65,70]. The activation of G-proteins in turn initiate a chain of reactions beginning with adenylate cyclase, cAMP, and protein ki-

nases that ultimately result in increased phosphorylation of various substrates. G-proteins are involved in the regulation of ion channels, metabolism, gene expression, and cytoskeletal structures via second messenger systems. A variety of mechanisms have been proposed by which Al may alter the neuronal cytoskeleton [26,27,53,65,66,73,74,79].

The deposition of Al in the cerebrovasculature, may also contribute to the observed neuronal injury by altering the BBB or cerebral blood flow. Examination of the immunoreactivity of IgM in the brain revealed that both AIF₃ and NaF groups had increased levels of IgM in the cortex of the right hemisphere as compared to the controls. Serum proteins, such as IgM and other antibodies, are typically excluded from neuronal tissue by the BBB [8,9]. The increased immunoreactivity of IgM in the present study may be indicative of a compromise in the BBB, consistent with the observation that Al-chloride (10–100 mg kg⁻¹, i.v.) can alter the BBB of mice possibly through changes in lipophilicity or potentiation of existing transport mechanisms [5,6].

There are striking parallels between Al-induced alterations in cerebrovasculature those associated with Alzheimer's disease (AD) and other forms of dementia. Alteration in the BBB can also promote inflammation involving activated microglia which may be preferentially associated with the amyloid plaques in AD [2,11,45,62,63]. Brain capillaries of patients with AD and of many aged individuals are found to be distorted and often contain amyloid deposits; the primary cause of these distortions is unknown [3,15,31,32]. These capillary distortions can disrupt blood flow patterns, altering cerebral metabolism and if sustained, contribute to progressive degeneration of neurons. Studies of AD and other dementing disorders have shown that microvascular abnormalities display a regional and laminar specificity in accordance with neuronal degeneration patterns, suggesting that the alterations in the cerebrovasculature may be a primary event in neurodegenerative disease [11]. Accumulation of β -amyloid has been found in the cerebrovasculature and spinal cord vasculature of elderly persons both those with and without AD. The deposition seems to be correlated with age and may be a direct consequence of the development of blood vessel abnormalities [31,37,38]. Vascular tissue produces β -amyloid and the vascular deposition of amyloid may result from alterations in the basement membrane of blood vessels that frequently occur with aging [36,37]. Whether amyloid is a causative factor in neurodegeneration [28,29,62,63] or a secondary consequence of injury [31,40,43,57], Al appears to have the capacity to influence the distribution and properties of amyloid [7,12,16,18,20,21,40,43,55,63,67]. In the present study animals in both the AIF₃ and NaF groups exhibited a bimodal distribution of vascular β -amyloid in both hemispheres of the lateral posterior thalamus, it was either absent or present in high levels in both treated groups. This increase

in vascular amyloid thalamus may be causally related to the neuronal degeneration found in its major target, the superior parietal cortex. In contrast, the control group expressed consistently only low levels of immunostaining—a unimodal distribution. While the presence of low levels of β -amyloid in the controls may be the result of a natural continuing, but limited, production of the protein throughout life [31,63], the bimodal distribution of β -amyloid in our AIF₃ and NaF-treated rats, however, remains a puzzle.

While the present results do not address the causal mechanisms of Al-induced neural degeneration, they do demonstrate that ingested Al reaches the brain, and in such animals there exists evidence of neural injury. While the small amount of AIF₃ in the drinking water of rats required for neurotoxic effects is surprising, perhaps even more surprising are the neurotoxic results of NaF at the dose given in the present study (2.1 ppm). Since dietary sources of F are additive in animals [44,46,69]; perhaps for the animals in the NaF group, the F in their chow together with their drinking water exceeded tolerable levels. F has diverse actions on a variety of cellular and physiological functions including the inhibition of a variety of enzymes, a corrosive action in acid mediums, hypocalcemia, hyperkalemia, and perhaps cerebral impairment [5,46,69]. Few chronic toxicity studies of F, however, have included extensive histological characterization of injury to the brain. In most reports of chronic F toxicity, the data provided are usually limited to weight loss, dental and skeletal changes, indicators of carcinogenesis, and damage to soft tissues [10,17,44,56,68,81]. The results of the present study indicate that more intensive neuropathological evaluations of F effects on brain may prove to be of value.

In summary, chronic administration of AIF₃ and NaF in the drinking water of rats resulted in distinct morphological alterations in the brain, including effects on neurons and cerebrovasculature. Further studies of AIF₃ and NaF are needed to establish the relative importance of a variety of potential mechanisms contributing to the observed effects as well as to determine the potential involvement of these agents in neurodegenerative diseases.

Acknowledgements

Acknowledgement We wish to thank Dr. Gustavo Reynoso for examination of pathological tissues and his valuable discussion and suggestions. We also wish to thank Obeda Lavin and Jeanene Olin for their histological expertise. This document has been reviewed by the National Health and Environmental Effects Research Laboratory of the US Environmental Protection Agency but the views expressed may not necessarily reflect agency policy and mention of trade names or commercial products does not constitute endorsement or recommendation for use.

References

- [1] H.W. Ahn, B. Fulton, D. Moxon, E.H. Jeffery, Interactive effects of fluoride and aluminum uptake and accumulation in bones of rabbits administered both agents in their drinking water, *J. Toxicol. Environ. Health* 44 (1995) 337–350.
- [2] P.S. Aisen, K.L. Davis, Inflammatory mechanisms in Alzheimer's disease: implications for therapy, *Am. J. Psychiatry* 151 (1994) 1105–1113.
- [3] R.A. Armstrong, Is the clustering of beta-amyloid (A beta) deposits in the frontal cortex of Alzheimer patients determined by blood vessels?, *Neurosci. Lett.* 195 (1995) 121–124.
- [4] R.A. Armstrong, S.J. Winsper, J.A. Blair, Aluminium and Alzheimer's disease: review of possible pathogenic mechanisms, *Dementia* 7 (1996) 1–9.
- [5] W.L. Augenstein, D.G. Spoerke, K.W. Kulig, A.H. Hall, P.K. Hall, B.S. Riggs, M.E. Saadi, B.M. Rumack, Fluoride ingestion in children: A review of 87 cases, *Pediatrics* 88 (1991) 907–912.
- [6] W.A. Banks, A.J. Kastin, Aluminum alters the permeability of the blood-brain barrier to some non-peptides, *Neuropharmacology* 24 (1985) 407–412.
- [7] W.A. Banks, L.M. Maness, M.F. Banks, A.J. Kastin, Aluminum-sensitive degradation of amyloid beta-protein 1-40 by murine and human intracellular enzymes, *Neurotoxicol. Teratol.* 18 (1996) 671–677.
- [8] E. Benjami, S. Leskowitz, *Immunology: A Short Course*, Wiley-Liss, New York, 1991.
- [9] H.G. Bluestein, N.J. Zvaifler, Antibodies reactive with central nervous system antigens, *Hum. Pathol.* 14 (1983) 424–428.
- [10] E. Braunwald, K.J. Isselbacher, R.G. Petersdorf, J.D. Wilson, J.B. Martin, A.S. Fauci, *Harrison's Principles of Internal Medicine*. McGraw-Hill, New York, 1987.
- [11] L. Buee, P.R. Hof, C. Bouras, A. Delacourte, D.P. Perl, J.H. Morrison, H.M. Fillit, Pathological alterations of the cerebral microvasculature in Alzheimer's disease and related dementing disorders, *Acta Neuropathol.* 87 (1994) 469–480.
- [12] Y.H. Chong, Y.H. Suh, Aggregation of amyloid precursor proteins by aluminum in vitro, *Brain Res.* 670 (1995) 137–141.
- [13] D.R. Crapper, A.J. Dalton, Aluminum induced neurofibrillary degeneration, brain electrical activity, and alterations in acquisition and retention, *Physiol. Behav.* 10 (1973) 935–945.
- [14] U. De Boni, J.W. Scott, D.R. Crapper, Intracellular aluminum binding: A histochemical study, *Histochem. J.* 40 (1974) 31–37.
- [15] J.C. De La Torre, Impaired brain microcirculation may trigger Alzheimer's disease, *Neurosci. Biobehav. Rev.* 18 (1994) 397–407.
- [16] J.L. Domingo, Adverse effects of aluminium-chelating compounds for clinical use, *Adverse Drug React. Toxicol. Rev.* 15 (1996) 145–165.
- [17] R.Y. Eagers, *Toxic Properties of Inorganic Fluorine Compounds*. Elsevier, Amsterdam, 1986.
- [18] C. Exley, Amyloid, aluminum and the etiology of Alzheimer's disease, *Med. J. Aust.* 164 (1996) 252–253, letter; comment.
- [19] C. Exley, E. Burgess, J.P. Day, E.H. Jeffery, S. Melethil, R.A. Yokel, Aluminum toxicokinetics, *J. Toxicol. Environ. Health* 48 (1996) 569–584.
- [20] C. Exley, N.C. Price, S.M. Kelly, J.D. Birchall, An interaction of beta-amyloid with aluminum in vitro, *FEBS Lett.* 324 (1993) 293–295.
- [21] G.D. Fasman, A. Perczel, C.D. Moore, Solubilization of beta-amyloid-(1-42)-peptide: reversing the beta-sheet conformation induced by aluminum with silicates, *Proc. Natl. Acad. Sci. USA* 92 (1995) 369–371.
- [22] J. Fleming, J.G. Joshi, Ferritin: isolation of aluminum–ferritin complex from the brain, *Proc. Natl. Acad. Sci. USA* 84 (1987) 7866–7870.
- [23] W.F. Forbes, L.M. Hayward, N. Agwani, Dementia, aluminium, and fluoride, *Lancet* 338 (1991) 1592–1593, letter; comment.
- [24] W.F. Forbes, D.R. McLachlan, Further thoughts on the aluminum–Alzheimer's disease link, *J. Epidemiol. Community Health* 50 (1996) 401–403.
- [25] B. Fulton, S. Jaw, E.H. Jeffery, Bioavailability of aluminum from drinking water, *Fundam. Appl. Toxicol.* 12 (1989) 144–150.
- [26] S. Gaytan-Garcia, H. Kim, M.J. Strong, Spinal motor neuron neuroaxonal spheroids in chronic aluminum neurotoxicity contain phosphatase-resistant high molecular weight neurofilament (NFH), *Toxicology* 108 (1996) 17–24.
- [27] T. Gotow, J. Tanaka, M. Takeda, The organization of neurofilaments accumulated in perikaryon following aluminum administration: relationship between structure and phosphorylation of neurofilaments, *Neuroscience* 64 (1995) 553–569.
- [28] J.A. Hardy, Anatomical cascade hypothesis for Alzheimer's disease, *TINS* 15 (1992) 200–201.
- [29] J.A. Hardy, G.A. Higgins, Alzheimer's disease: the amyloid cascade hypothesis, *Science* 256 (1992) 184–185.
- [30] W.R. Harris, G. Berthon, J.P. Day, C. Exley, T.P. Flaten, W.F. Forbes, T. Kiss, C. Orvig, P.F. Zatta, Speciation of aluminum in biological systems, *J. Toxicol. Environ. Health* 48 (1996) 543–568.
- [31] M.N. Hart, J. Bennett-Gray, A.H. Menezes, J.A. Goeken, R.L. Schelper, H.M. Wisniewski, Beta-amyloid protein of Alzheimer's disease is found in cerebral and spinal cord vascular malformations, *Am. J. Pathol.* 132 (1988) 167–172.
- [32] O. Hassler, Arterial deformities in senile brains, *Acta Neuropathol.* 8 (1967) 219–229.
- [33] R.F. Itzhaki, Possible factors in the etiology of Alzheimer's disease, *Mol. Neurobiol.* 9 (1994) 1–13.
- [34] M. Jacqmin, D. Commenges, L. Letenneur, P. Barberger-Gateau, J.F. Dartigues, Components of drinking water and risk of cognitive impairment in the elderly, *Am. J. Epidemiol.* 139 (1994) 48–57.
- [35] G.V.W. Johnson, R.S. Jope, Aluminum alters cyclic AMP and cyclic GMP levels but not presynaptic cholinergic markers in rat brain in vivo, *Brain Res.* 403 (1987) 1–6.
- [36] R.N. Kalaria, A.B. Pax, Increased collagen content of cerebral microvessels in Alzheimer's disease, *Brain Res.* 705 (1995) 349–352.
- [37] R.N. Kalaria, D.R.D. Premkumar, A.B. Pax, D.L. Cohen, I. Lieberburg, Production and increased detection of amyloid B protein and amyloidogenic fragments in brain microvessels, meningeal vessels, and choroid plexus in Alzheimer's disease, *Brain Res. Mol. Brain Res.* 35 (1996) 58–68.
- [38] L.S. Kaminsky, M.C. Moheny, J. Leach, J. Melius, M.J. Miller, Fluoride: benefits and risks of exposure, *Crit. Rev. Oral Biol. Med.* 1 (1990) 261–281.
- [39] Y. Kanaho, J. Moss, M. Vaughn, Mechanism of inhibitors of transducin GTPase activity by fluoride and aluminum, *J. Biol. Chem.* 260 (1985) 11493–11497.
- [40] M. Kawahara, K. Muramoto, K. Kobayashi, H. Mori, Y. Kuroda, Aluminum promotes the aggregation of Alzheimer's amyloid beta-protein in vitro, *Biochem. Biophys. Res. Commun.* 198 (1994) 531–535.
- [41] T. Kiamoto, K. Ogomori, J. Tateishi, S.B. Prusiner, Formic acid pretreatment enhances immunostaining of cerebral and systemic amyloids, *Lab. Invest.* 57 (1987) 230–236.
- [42] A.S. Kraus, W.F. Forbes, Aluminum, fluoride and the prevention of Alzheimer's disease, *Can. J. Public Health* 83 (1992) 97–100.
- [43] Y. Kuroda, M. Kawahara, Aggregation of amyloid beta-protein and its neurotoxicity: enhancement by aluminum and other metals, *Tohoku. J. Exp. Med.* 174 (1994) 263–268.
- [44] L.R. McDowell, *Minerals in Animal and Human Nutrition*. Academic Press, San Diego, 1992.
- [45] P.L. McGeer, E.G. McGeer, The inflammatory response system of brain: Implications for therapy of Alzheimer and other neurodegenerative diseases, *Brain Res. Rev.* 21 (1995) 195–218.
- [46] M.E. McIvor, Acute fluoride toxicity, *Drug Safety* 5 (1997) 79–85.
- [47] D.R. McLachlan, C. Bergeron, J.E. Smith, D. Boomer, S.L. Rifat, Risk for neuropathologically confirmed Alzheimer's disease and

- residual aluminum in municipal drinking water employing weighted residential histories, *Neurology* 46 (1996) 401–405, See comments.
- [48] D.R. McLachlan, J. Massiah, Aluminum ingestion: a risk factor for Alzheimer's disease, in: R.L. Isaacson, K.F. Jensen (Eds.), *The Vulnerable Brain and Environmental Risks: Toxins in Food*, Vol. 2. Plenum, New York, 1992, pp. 49–50.
- [49] C.M. Morris, A.B. Keith, J.A. Edwardson, R.G.L. Pullen, Uptake and distribution of iron and transferrin in the adult rat brain, *J. Neurochem.* 59 (1992) 300–305.
- [50] W.R. Mundy, T. Freudenrich, T.J. Shafer, A.C. Nostrandt, In vitro aluminum inhibition of brain phosphoinositide metabolism: comparison of neonatal and adult rats, *Neurotoxicology* 16 (1995) 35–44.
- [51] W.R. Mundy, P.R. Kodavanti, V.F. Dulchinos, H.A. Tilson, Aluminum alters calcium transport in plasma membrane and endoplasmic reticulum from rat brain, *J. Biochem. Toxicol.* 9 (1994) 17–23.
- [52] L.C. Neri, D. Hewitt, Aluminum, Alzheimer's disease, and drinking water, *Lancet* 338 (1991) 390.
- [53] R.A. Nixon, J.F. Clarke, K.B. Logvinenko, M.K. Tan, M. Hoult, F. Grynspan, Aluminum inhibits calpain-mediated proteolysis and induces human neurofilament proteins to form protease-resistant high molecular weight complexes, *J. Neurochem.* 55 (1990) 1950–1959.
- [54] A.C. Nostrandt, T.J. Shafer, W.R. Mundy, S. Padilla, Inhibition of rat brain phosphatidylinositol-specific phospholipase C by aluminum: regional differences, interactions with aluminum salts, and mechanisms, *Toxicol. Appl. Pharmacol.* 136 (1996) 118–125.
- [55] S.R. Paik, J.H. Lee, D.H. Kim, C.S. Chang, J. Kim, Aluminum-induced structural alterations of the precursor of the non-A beta component of Alzheimer's disease amyloid, *Arch. Biochem. Biophys.* 344 (1997) 325–334.
- [56] M.G. Paranjpe, A.M. Chandra, C.W. Qualls Jr., S.T. McMurry, M.D. Rohrer, M.M. Whaley, R.L. Lochmiller, K. McBee, Fluorosis in a wild cotton rat (*Sigmodon hispidus*) population inhabiting a petrochemical waste site, *Toxicol. Pathol.* 22 (1994) 569–578.
- [57] A.D. Roses, Apolipoprotein E affects the rate of Alzheimer's disease expression: Beta-amyloid burden is a secondary consequence dependent on APOE genotype and duration of disease, *J. Neuropathol. Exp. Neurol.* 53 (1994) 429–437.
- [58] A.J. Roskams, J.R. Connor, Aluminum access to the brain: A role for transferrin and its receptor, *Proc. Natl. Acad. Sci. USA* 87 (1990) 9024–9027.
- [59] E.M. Ross, G-proteins and receptors in neuronal signalling, in: Z.W. Hall (Ed.), *An Introduction to Molecular Neurobiology*. Sinauer Assoc., MA, 1992, pp. 181–206.
- [60] E. Salib, V. Hillier, A case-control study of Alzheimer's disease and aluminium occupation, *Br. J. Psychiatry* 168 (1996) 244–249.
- [61] J.C. Schroeder, P.E. Tolbert, E.A. Eisen, R.R. Monson, M.F. Hallock, T.J. Smith, S.R. Woskie, S.K. Hammond, D.K. Milton, Mortality studies of machining fluid exposure in the automobile industry: IV. A case-control study of lung cancer, *Am. J. Ind. Med.* 31 (1997) 525–533.
- [62] D.J. Selkoe, Physiological production of the beta-amyloid protein and the mechanism of Alzheimer's disease, *TINS* 16 (1993) 403–409.
- [63] D.J. Selkoe, Alzheimer's disease: A central role for amyloid, *J. Neuropathol. Exp. Neurol.* 53 (1994) 438–447.
- [64] T.J. Shafer, W.R. Mundy, Effects of aluminum on neuronal signal transduction: mechanisms underlying disruption of phosphoinositide hydrolysis, *Gen. Pharmacol.* 26 (1995) 889–895.
- [65] T.B. Shea, Calcium modulates aluminum neurotoxicity and interaction with neurofilaments, *Mol. Chem. Neuropathol.* 24 (1995) 151–163.
- [66] T.B. Shea, T. Husain, Inhibition of proteolysis enhances aluminum-induced perikaryal neurofilament accumulation but does not enhance tau accumulation, *Mol. Chem. Neuropathol.* 26 (1995) 195–212.
- [67] K. Shigematsu, P.L. McGeer, Accumulation of amyloid precursor protein in damaged neuronal processes and microglia following intracerebral administration of aluminum salts, *Brain Res.* 593 (1992) 117–123.
- [68] J.L. Shupe, R.H. Bruner, J.L. Seymour, C.L. Alden, The pathology of chronic bovine fluorosis: A review, *Toxicol. Pathol.* 20 (1992) 274–288.
- [69] B. Spittle, Psychopharmacology of fluoride: A review, *Int. Clin. Psychopharmacol.* 9 (1994) 79–82.
- [70] P.C. Sternweis, A.G. Gilman, Aluminum: A requirement for activation of the regulatory component of adenylate cyclase by fluoride, *Proc. Natl. Acad. Sci. USA* 79 (1982) 4888–4891.
- [71] C.N. Still, Aluminum neurotoxicity and Alzheimer's disease, *J.S.C. Med. Assoc.* 90 (1994) 560–564.
- [72] E. Storey, C.L. Masters, Amyloid, aluminium and the etiology of Alzheimer's disease, *Med. J. Aust.* 163 (1995) 256–259.
- [73] M.J. Strong, Aluminum neurotoxicity: An experimental approach to the induction of neurofilamentous inclusions, *J. Neurol. Sci.* 124 (1994) 20–26, Suppl.
- [74] M.J. Strong, K. Mao, V.R. Nerurkar, I. Wakayama, R. Yanagihara, R.M. Garruto, Dose-dependent selective suppression of light (NFL) and medium (NFM) but not heavy (NFH) molecular weight neurofilament mRNA levels in acute aluminum neurotoxicity, *Mol. Cell Neurosci.* 5 (1994) 319–326.
- [75] G.A. Taylor, A.J. Newens, J.A. Edwardson, D.W. Kay, D.P. Forster, Alzheimer's disease and the relationship between silicon and aluminium in water supplies in northern England, *J. Epidemiol. Community Health* 49 (1995) 323–324, See comments.
- [76] E. Trimmer, Aluminium and Alzheimer's disease in Finchley, north London, *Lancet* 344 (1994) 486, letter; comment.
- [77] J.A. Varner, W.J. Horvath, C.W. Huie, H.R. Naslund, R.L. Isaacson, Chronic aluminum fluoride administration: I. Behavioral observations, *Behav. Neural Biol.* 61 (1994) 233–241.
- [78] J.A. Varner, C.W. Huie, W. Horvath, K.F. Jensen, R.L. Isaacson, Chronic AlF_3 administration: II. Selected histological observations, *Neurosci. Res. Comm.* 13 (1993) 99–104.
- [79] I. Wakayama, V.R. Nerurkar, M.J. Strong, R.M. Garruto, Comparative study of chronic aluminum-induced neurofilamentous aggregates with intracytoplasmic inclusions of amyotrophic lateral sclerosis, *Acta Neuropathol.* 92 (1996) 545–554.
- [80] J.R. Walton, Amyloid, aluminium and the etiology of Alzheimer's disease, *Med. J. Aust.* 164 (1996) 382–383.
- [81] G.M. Whitford, Acute and chronic fluoride toxicity, *J. Dent. Res.* 71 (1992) 1249–1254.
- [82] N. Wu, W.J. Horvath, C.W. Huie, Speciation of inorganic aluminum using capillary zone electrophoresis with indirect UV detection, *J. Chromatogr.* 635 (1993) 307–312.